Preparation and Characterization of Some Esters Impregnated with Magnetic Iron Oxide Nanoparticles Fe_3O_4 and Study of Their Efficiency in for Adsorption of Lead Ions from Their Aqueous Solutions

Jaafar S. Jaafar[1,*], Ali A. Abdulwahid[2], Yosra A. Maarch[2]

`1. Marine Inspection Department, Environment sector, General Company for Ports of Iraq (GCPI), Basra, Iraq.

2. Department of Chemistry, College of Science, University of Basrah, Basra, Iraq

*Corresponding author, E-mail: **jaafarsd2020@yahoo.com**

Doi:10.29072/basjs.202128

Abstract

Lead is a naturally occurring toxic metal found in the earth's crust. Its widespread use has resulted in extensive environmental contamination, human exposure and significant public health problems in many parts of the world. In this study we report the preparation of three esters impregnated with magnetic nanoparticles Fe_3O_4, esters prepared from 2,2-bis(hydroxyl methyl)propane-1,3-diol with 4-hydroxy benzoic acid (I), nicotinic acid (niacin) (II) and stearic acid (III). The synthesis absorbents (I@Fe_3O_4, II@Fe_3O_4 and III@Fe_3O_4) proved to be effective for the removal of lead ions from aqueous solution at near-neutral pH, the adsorption behavior was matching with Langmuir model for I@Fe_3O_4 and II@Fe_3O_4 and in keeping with Freundlich model for III@Fe_3O_4 with q_{max} values of 862.068 mg/g, 1149.425 mg/g and 261.096 mg/g respectively. The adsorption of Pb(II) follows pseudo-first-order kinetics for three adsorbents.

Article inf.

Received: *21/6/2021*

Accepted: *12/8/2021*

Published: *31/8/2021*

keywords:

Esters impregnated, iron oxide, Fe_3O_4 nanoparticles

This article is an open access article distributed under the terms and conditions of the Creative Commons Attribution-NonCommercial 4.0 International (CC BY-NC 4.0 license) (http://creativecommons.org/licenses/by-nc/4.0/).

1. Introduction

Heavy elements are known as the elements whose density is more than five times the density of water [1] , as they have atomic weights between 63.5 to 200.6, and a specific weight of more than 5 gm / cm^3 [2] and have negative effects when they are overused, and these elements are present Naturally occurring in the soil of the land but increased due to the increase in industrial, domestic, agricultural, medical and technological activities. Lead is one of the most important heavy elements with negative effects on humans and the environment, and is classified as the second most toxic substance in the list of hazardous compounds [3] due to the high level of toxicity. It is a plastic metal, used in the manufacture of electrical cables, water pipes , paints and pesticides . For continuous exposure to it on a wide range of harmful health effects for both adults and children , the World Health Organization (WHO) and the European Union (EU) have determined its percentage in drinking water to be no more than 0.01 mg L^{-1} [4]. As for the nanoparticles, they are known as an atomic or molecular grouping whose number ranges from a few atoms (or molecules) to a million atoms, linked to each other in an almost spherical form, having a radius of less than 100 nanometers. Nanomaterials have the advantage that they have a larger surface area when compared to the same mass of larger materials , and this makes them more chemically active. Very few atoms are present on the surface compared to those on the inside.

Adsorption is one of the most common methods in water treatment, as adsorption has received great attention in the science of removing pollutants due to the high efficiency of this technology, ease of operation, ability to regenerate materials , amla and flexibility in design. The adsorption of lead (II) ions onto the prepared esters impregnated with Fe_3O_4 were investigated with variations in the parameters of pH, contact time, lead (II) ions concentration and temperature. The kinetic model for lead (II) adsorption onto the prepared esters impregnated with Fe_3O_4 was also studied .

2. Experimental

2.1. Materials

Solid and liquid chemical materials from different origins were used. Three different carboxylic acids were used to prepare the esters, which are 4-hydroxy benzoic acid from Merck, Nicotinic acid from CDH company and Stearic acid from Fluka company in addition to the alcoholic compound 2,2-bis(hydroxyl methyl)propane-1,3-diol from Sigma Aldrich company and used anhydrous ferric chloride ($FeCl_3$) from Sigma Aldrich company, Ammonium ferrous sulphate

This article is an open access article distributed under the terms and conditions of the Creative Commons Attribution-NonCommercial 4.0 International (CC BY-NC 4.0 license) (http://creativecommons.org/licenses/by-nc/4.0/).

hexahydrate $(NH_4)_2SO_4.FeSO_4.6H_2O$ from G.P.R company, Lead nitrate (Blei(II)-nitrat) from BDH company to prepare solutions of elemental lead , triphenylphosphine (ph_3P) from Fluka and tri ethyl amine from Merck. In addition, a group of alcoholic solvents such as methanol and ethanol , bases , acids such as nitric acide and hydrochloric acide.

2.2. Preparation of Iron oxide magnetic nanoparticles

The (Fe_3O_4) ferromagnetic nanoparticles were prepared by Co - Precepetation , Fe^{+3} and Fe^{+2} with ammonium hydroxide solution , according to [5,6

$$Fe^{2+} + 2Fe^{3+} + 8OH^- \rightarrow Fe_3O_4 + 4H_2O \quad \ldots\ldots\ldots\ldots\ldots(1)$$

A 10 mmol (1.6220 gm) of anhydrous ferric chloride $(FeCl_3)$ and 5 mmol (1.9608 gm) of ammonium ferrous sulfate $(NH_4)_2SO_4.FeSO_4.6H_2O$ were dissolved in 150 ml of anionic distilled water, in a 500 ml flask with continuous stirring of this solution using hot plate with magnetic sterrir with heating to a temperature of 90°C , where the chemical precipitation magnetic iron particles (Fe_3O_4) were added by adding 50ml of a solution of 32% ammonium hydroxide NH_4OH in the form of droplets with continuous stirring until the pH function reached 10.0 - 10.5, the color of the solution changed from brown to dark black and black precipitate was separated using an external magnet where the Fe_3O_4 particles formed at the bottom of the beaker adjacent to the magnet were collected while the color of the solution remained above it transparent indicating completeness. Then separating the sediment from the filtrate by the decantation process with the help of an external magnet and washing by 10% deionized distilled water with methanol therefore, several times until the excess was removed from the ammonium hydroxide solution and the pH function of the wash water became neutral, the sediment was completely dried from the washing water.

2.3 Preparation of esters [7]

Esters were prepared using three different carboxylic acids , 4-hydroxy benzoic acid , nicotinic acid (niacin) , and stearic acid , by reacting with the alcoholic compound 2,2-bis (hydroxyl methyl) propane-1,3-diol . In 250 ml flask 6mmol (1.560 gm) of TriPhenyl Phosphine (ph_3P) were mixed with 6 mmol (1.520 gm) of iodine I_2, in the presence of 25 ml of dichloro methane (CH_2Cl_2) as solvent with continuous stirring with a magnetic stirrer device , then added,

This article is an open access article distributed under the terms and conditions of the Creative Commons Attribution-NonCommercial 4.0 International (CC BY-NC 4.0 license) (http://creativecommons.org/licenses/by-nc/4.0/).

4 mmol of carboxylic acid to the mixture followed by adding 3.70 mmol (2 ml) of triethyl amine with continued shaking for 5 minutes at room temperature after which 1.50 mmol (0.204 gm) was added to reaction of the 2,2-bis (hydroxyl methyl) propane-1,3-diol, The mixing was completed for 30 min a light brown sticky solid was formed , it was washed several times with diethyl ether and the washing residues were disposed of by decantation and then the powders formed were transferred to filter paper No. 40, it was washed several times with ether, then with anionic distilled water to get rid of the excess of carboxylic acid and alcohol, and left to dry, as an off-white powder was formed, the reaction was followed up by means of a thin layer chromatography test, where the values of R_f = 0.7 , 0.7 and 0.6 respectively, and the melting point of the three prepared esters (I , II , III) were equal to 140-143°C , 135 - 137°C and 112 - 114°C respectively, they differ from the melting points of carboxylic acids and alcohols that form esters.

2.4 Preparation of the adsorbents

The ferromagnetic nanoparticles were mixed with the prepared esters (I , II and III) separately and at a mixing ratio of 1:1 (w/w) , where equal weights were taken from each of the magnetic iron nanoparticles and esters (I , II , III) transformed into 25ml of ionic distilled water in 100 ml flask and left for 30min. in Ultra sonacation device, after that the two solutions were mixed well and left again in ultrasound machine for three hours, then left until they were completely dry for next adsorption study. The prepared adsorbents I@Fe_3O_4 , II@Fe_3O_4 and III@Fe_3O_4 were characterized by field emission scanning electron microscopy (FESEM) and transmission electron microscopy (TEM) technology , figures (6) – (11) show the prepared adsorbents .

2.5 Effect of pH

The effect of pH on the lead (II) ion adsorption capacity of absorbents (I@Fe_3O_4 , II@Fe_3O_4 and III@Fe_3O_4) was studied at (300 mg L^{-1} , 400 mg L^{-1} and 100 mg L^{-1}) respectively initial lead (II) ion concentration and at 20°C. The pH of solutions is a factor which plays an important role in the adsorption process . Because lead (II) ions precipitate as lead (II) hydroxide at pH values higher than 6.5[8], above this pH value adsorption experiments were not carried out.

2.6. Adsorption Experiments.

This article is an open access article distributed under the terms and conditions of the Creative Commons Attribution-NonCommercial 4.0 International (CC BY-NC 4.0 license) (http://creativecommons.org/licenses/by-nc/4.0/).

The adsorption experiments were done in a batch system . Certain amount of absorbent (I@Fe_3O_4 , II@Fe_3O_4 and III@Fe_3O_4) was added to a lead (II) nitrate solution in an Erlenmeyer flask closed with a glass stopper and the flask content stirred using a magnetic stirrer at 200 rpm to determine the optimum values of pH, initial concentration of lead (II) ions. A stock solution containing 1000 mg / L of lead (II) ions was used for the adsorption experiments . The required lead (II) concentrations were provided with the dilution using deionized water. 100 mL of a lead (II) solution containing 0.05 g of the adsorbent in a 100 mL stopper conical flask was agitated at 200 rpm in a water bath , of which temperature was controlled at desired temperature (20°C , 40°C and 65°C). The lead (II) ions concentration of the solution was determined by Flame Atomic Absorption Spectroscopy (AAS) model (Phoenix-986 AA Spectrophotometer) . The amount of lead (II) ions on the adsorbent at equilibrium was determined from the difference between the initial and final concentrations of the lead (II) solutions.

3. Results and Discussions

3.1 FESEM and TEM test.

Field Emission Scanning Electron Microscopy Images (FESEM) and Transmission Electron Microscopy (TEM) for prepared Fe_3O_4 nanoparticles and I@Fe_3O_4 , II@Fe_3O_4 and III@Fe_3O_4 showed in Figs. 1&2.

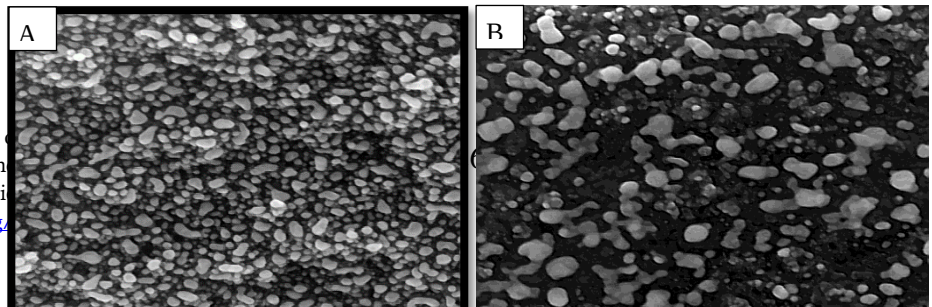

This article is an
the terms and conditions of th
NonCommercial 4.0 Internati
(http://creativecommons.org/

Figure 1 : FESEM images for (A) Fe_3O_4, (B) I@Fe_3O_4, (C) II@Fe_3O_4, and (D) III@Fe_3O_4

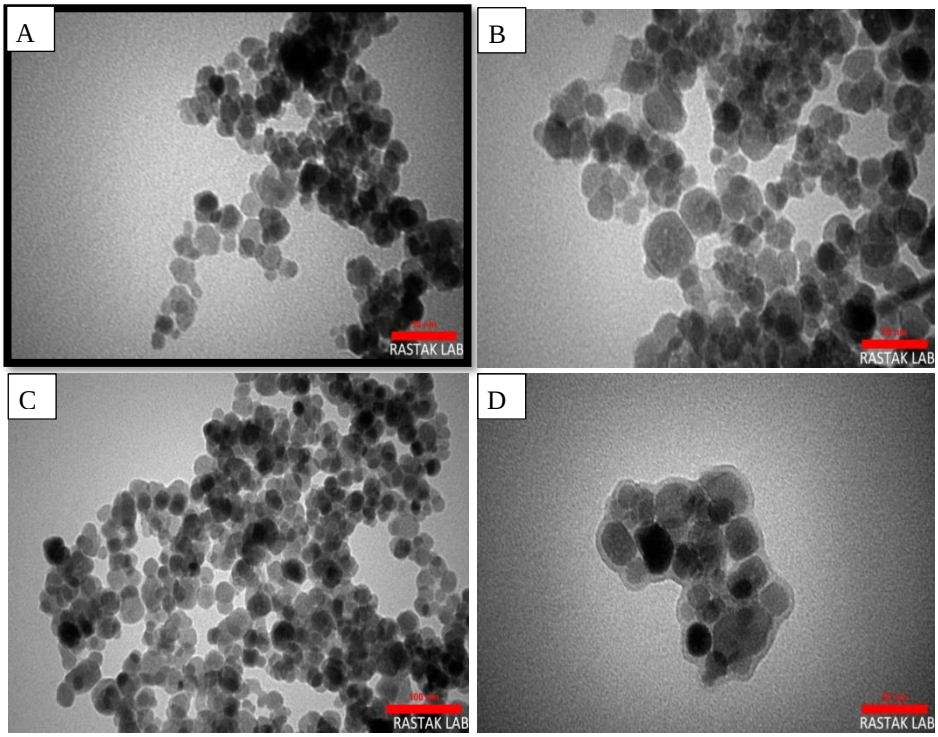

Figure 2 : TEM images for (A) Fe_3O_4, (B) I@Fe_3O_4, (C) II@Fe_3O_4, and (D) III@Fe_3O_4

3.2 FTIR and CHN Analysis

This article is an open access article distributed under the terms and conditions of the Creative Commons Attribution-NonCommercial 4.0 International (CC BY-NC 4.0 license) (http://creativecommons.org/licenses/by-nc/4.0/).

The prepared esters were diagnosed using Fourier transform Infrared spectroscopy technology (FTIR) as shown in the tables (1-3) and the technique of accurate analysis of the elements as in the Tables 1-4 .

Table 1: Position FTIR spectrum of esters I

Type of band	Wavenumber (cm^{-1})
=C-H bending out of plane	694.40 , 725.26 , 756.12 , 806.27 , 848.71 , 887.28
=C-H bending in plane	1010.73 , 1118.75
C-O-C $_{St\ sym}$	1053.17
C-O-C $_{St\ .asym}$	1203.62
C-O $_{St}$ of alcoholic	1157.33
OH bending	1265.35
C-H bending	1411.94 , 1438.94 , 1465.95
C=C $_{St}$ aromatic	1508.38 , 1600.97
C=O for ester	1739.85
Weak combination and overton	1750 – 2000
C-H $_{St\ .\ Sym}$ (CH_2)	2889.46
C-H $_{St\ .\ Asym}$ (CH_2)	2939.61
=C-H $_{St}$ (w)	3074.63
OH bonded	3333.10 , 3383.26 , 3406.40
Carbonyl overton band	3450

Table 2 : Position FTIR spectrum of esters II

This article is an open access article distributed under the terms and conditions of the Creative Commons Attribution-NonCommercial 4.0 International (CC BY-NC 4.0 license) (http://creativecommons.org/licenses/by-nc/4.0/).

Type of band	Wavenumber (cm^{-1})
=C-H bending out of plane	690.54 , 725.26 , 756.12 , 802.41 , 844.85 , 883.43
=C-H bending in plane	1018.45 , 1122.61
C-O-C $_{St\ sym}$	1060.88
C-O-C $_{St\ .asym}$	1207.48
C-N $_{St}$	1276.92
C-H bending	1419.66 , 1465.95
C=C $_{St}$ aromatic	1512.24 , 1600.97
C=N $_{St}$	1648.10
C=O for ester	1739.85
Weak combination and overton	1750 – 2000
C-H $_{St\ .\ Sym}$ (CH_2)	2881.75
C-H $_{St\ .\ Asym}$ (CH_2)	2935.76
=C-H $_{St}$	2966.62
Carbonyl overton band	3450

Table 3 : Position FTIR spectrum of esters III

Type of band	Wavenumber (cm^{-1})
C-C bending	698.25 , 725.26 , 756.12 , 806.27
C-O-C $_{St\ .\ Sym}$	1018.45 , 1118.75 , 1172.76
C=O $_{St}$ for ester	1743.71

This article is an open access article distributed under the terms and conditions of the Creative Commons Attribution-NonCommercial 4.0 International (CC BY-NC 4.0 license) (http://creativecommons.org/licenses/by-nc/4.0/).

C-H $_{St.Sym}$ (CH_2 , CH_3)	2850.88
C-H $_{St.Asym}$ (CH_2)	2920.32
C-H $_{St.Asym}$ (CH_3)	2997.48
Carbonyl overton band	3450

Table 4: CHN analysis of prepared esters

Ester type	M.wt	%C	%H	%N
I($C_{33}H_{28}O_{12}$)	616.58	64.28 / 64.12	4.58 / 4.13	0
II($C_{29}H_{24}N_4O_8$)	556.53	62.59 / 62.17	4.35 / 4.10	10.07 / 9.82
III($C_{77}H_{148}O_8$)	1201.12	76.94 / 76.34	12.41 / 12.13	0

3.3 Effect of pH

Adsorption capacity of adsorbents (I@Fe_3O_4 , II@Fe_3O_4 and III@Fe_3O_4) regarding the solution pH are illustrated in Figure 3 and Table 5. On the contrary, when the pH value increased , the electrostatic repulsion between lead (II) ions was decreased and the surface of absorbents (I@Fe_3O_4 , II@Fe_3O_4 and III@Fe_3O_4) became less positively charged, and the adsorption capacity of absorbents (I@Fe_3O_4 , II@Fe_3O_4 and III@Fe_3O_4) increased . Maximum adsorption capacity was found as 421mg g^{-1} , 566 mg g^{-1} and 124 mg g^{-1} at pH 6.0 respectively.

This article is an open access article distributed under the terms and conditions of the Creative Commons Attribution-NonCommercial 4.0 International (CC BY-NC 4.0 license) (http://creativecommons.org/licenses/by-nc/4.0/).

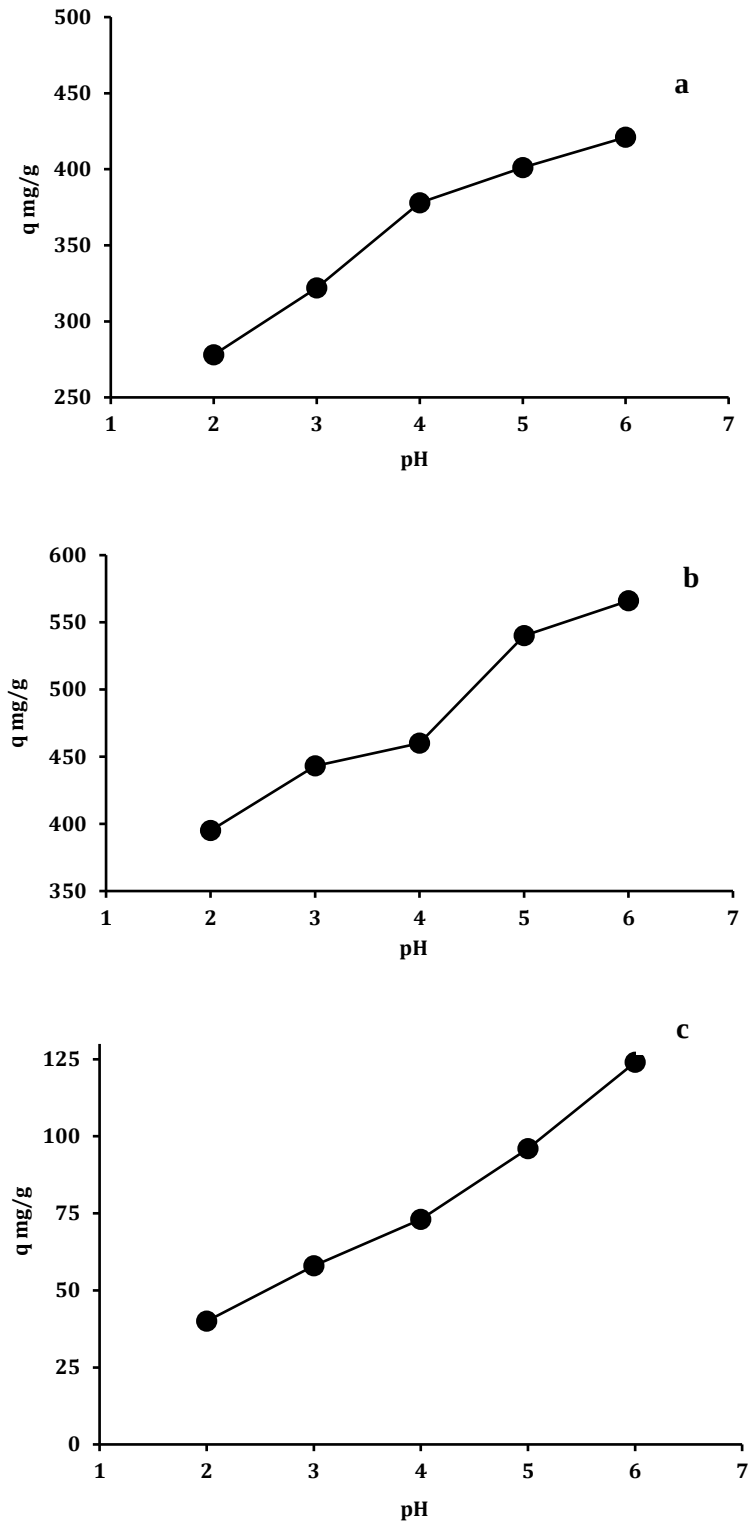

Figure 3: Effect of pH for the adsorption of lead (II) ions onto the (a) I@Fe_3O_4 , (b) II@Fe_3O_4 , (c) III@Fe_3O_4

($C_\circ$ = 100 mg L^{-1} , m = 0.05 g , V= 100 ml , T = 20°C , agitation rate 200 rpm)

This article is an open access article distributed under the terms and conditions of the Creative Commons Attribution-NonCommercial 4.0 International (CC BY-NC 4.0 license) (http://creativecommons.org/licenses/by-nc/4.0/).

Table 5: Optimization pH for adsorption of Pb(II) onto prepared adsorbents

Adsorbantion	Optimized pH - values		
	I@Fe_3O_4	II@Fe_3O_4	III@Fe_3O_4
Pb(II)	6.0	6.0	6.0

3.4 Effect of Contact Time

A series of contact time experiments for the adsorption of lead (II) ions onto adsorbents (I@Fe_3O_4 , II@Fe_3O_4 and III@Fe_3O_4) were carried out at the initial concentration of lead (II) ions (300 mg L^{-1} , 400 mg L^{-1} and 100 mg L^{-1}) respectively and temperatures of 20°C , 40°C and 65°C respectively . The effects of contact time on the adsorption process are shown in Fig.4. The adsorbed amount of lead (II) ions was increased with an increase in contact time up to 180 min, 120 min and 180 min respectively after that there was no significant increase in the adsorption of lead (II) ions onto adsorbents(I@Fe_3O_4 , II@Fe_3O_4 and III@Fe_3O_4), show the Table 6. At a 180 min , 120 min and 180 min respectively of contact time , the adsorbed amounts of lead (II) ions onto adsorbent (I@Fe_3O_4) were (407 , 504 and 590.15) mg g^{-1} at (20 , 40 and 65) °C respectively , adsorbent(II@Fe_3O_4) were (566 , 653 and 743) mg g^{-1} at (20 , 40 and 65) °C respectively and adsorbent (III@Fe_3O_4) were (117 , 157 and 184) mg g^{-1} at (20 , 40 and 65) °C respectively.

This article is an open access article distributed under the terms and conditions of the Creative Commons Attribution-NonCommercial 4.0 International (CC BY-NC 4.0 license) (http://creativecommons.org/licenses/by-nc/4.0/).

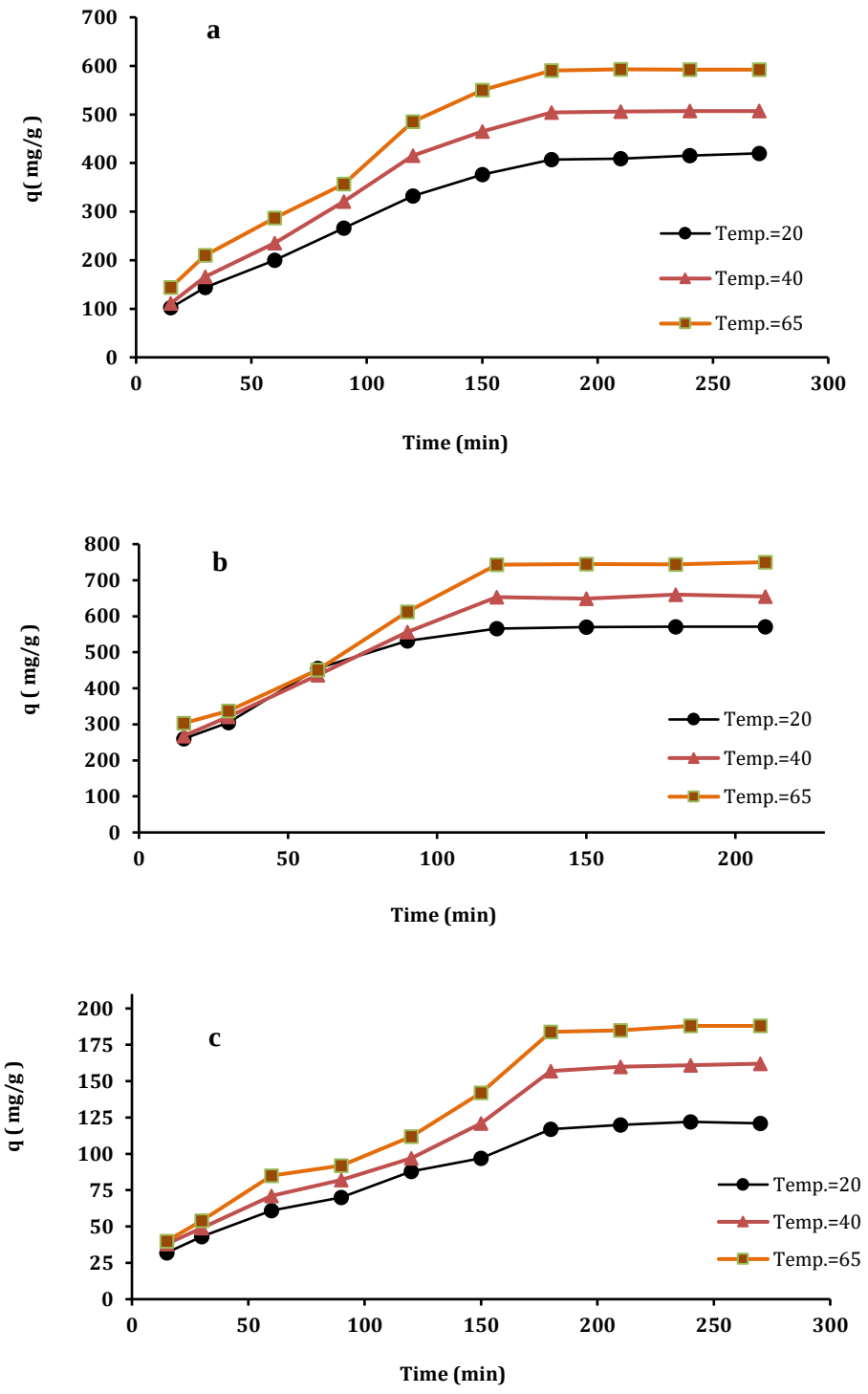

Figure 4: Effect of contact time for the adsorption of Pb(II) onto (a) I@Fe_3O_4 , (b) II@Fe_3O_4 , (c) III@Fe_3O_4

($C_\circ$ = 100 mg L^{-1} , m = 0.05 g , V= 100 ml , pH = 6.0 , agitation rate 200 rpm)

This article is an open access article distributed under the terms and conditions of the Creative Commons Attribution-NonCommercial 4.0 International (CC BY-NC 4.0 license) (http://creativecommons.org/licenses/by-nc/4.0/).

Table 6: The optimized contact time for adsorption of Pb(II) onto prepared adsorbents

adsorbant	Optimized contact time (min)		
	I@Fe_3O_4	II@Fe_3O_4	III@Fe_3O_4
Pb(II)	180	120	180

3.5 Effect of Initial Lead (II) Ions Concentration

The adsorption capacity of adsorbents (I@Fe_3O_4 , II@Fe_3O_4 and III@Fe_3O_4) for lead (II) ions was increased with an increase in the initial lead (II) ion concentration. This experiments were done by mixing constant weight of adsorbents and varying concentrations of lead (II) ion at optimum time and pH. Increases in the initial concentration of lead (II) ions cause the mass transfer from the aqueous phase to the solid phase. The maximum adsorption capacities were obtained at the initial lead (II) ion concentration of 300 mg L^{-1} , 400 mg L^{-1} and 100 mg L^{-1} respectively .

3.6 Adsorption Kinetics

To investigate the adsorption process of lead (II) ions onto adsorbents(I@Fe_3O_4 , II@Fe_3O_4 and III@Fe_3O_4) , the pseudo-first order kinetic[9] and pseudo-second-order kinetic[10] , were applied to the experimental data. The pseudo-first-order kinetic model equation is shown as :

$$\ln(q_e - q_t) = \ln q_1 - k_1 t \text{ .....(2)}$$

Where q_e and q_t are the amounts of lead (II) ions (mg g^{-1}) absorbed at equilibrium and at time t , respectively, and k_1 is the first-order rate constant (min^{-1}). Figure 5 showed pseudo-first-order kinetic model.

This article is an open access article distributed under the terms and conditions of the Creative Commons Attribution-NonCommercial 4.0 International (CC BY-NC 4.0 license) (http://creativecommons.org/licenses/by-nc/4.0/).

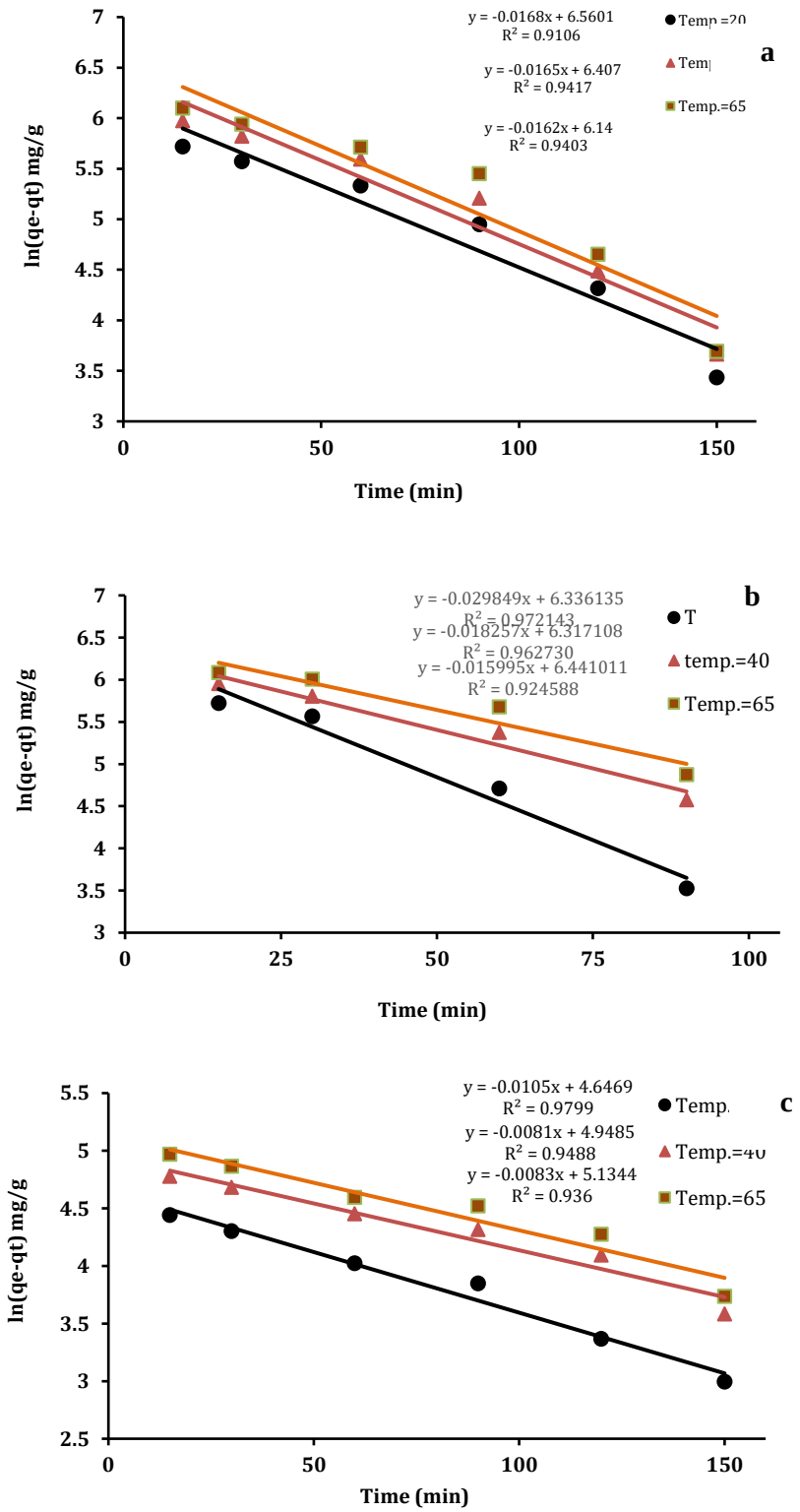

Figure 5: Pseudo – first – order kinetic plot for the adsorption of Pb(II) onto (a) I@Fe_3O_4 , (b) II@Fe_3O_4 , (c) III@Fe_3O_4 at different temp.

This article is an open access article distributed under the terms and conditions of the Creative Commons Attribution-NonCommercial 4.0 International (CC BY-NC 4.0 license) (http://creativecommons.org/licenses/by-nc/4.0/).

Table 7: Pseudo-First-Order parameters for adsorption of Pb(II) onto prepared adsorbents at different temperatures.

Absorbents	Temp. °C	Pb(II)		
		K_1	q_1	R_1^2
I@Fe_3O	20	0.0162	464.053	0.940
	40	0.0165	541.855	0.941
	65	0.0168	706.342	0.910
II@Fe_3O	20	0.0298	564.609	0.972
	40	0.018	553.953	0.962
	65	0.015	627.040	0.924
III@Fe_3O	20	0.010	104.261	0.979
	40	0.008	140.963	0.948
	65	0.008	169.762	0.936

K_1 : (min^{-1}) , q : (mg /g) , Temperature : (°C)

The pseudo-second-order kinetic model is shown as:

$$\frac{t}{q_t} = \frac{1}{K_2 q_2^2} + \frac{1}{q_2} t \quad \text{.....(3)}$$

where q_2 is the maximum adsorption capacity (mg g^{-1}) for the pseudo-second-order adsorption and k_2 is the equilibrium rate constant for pseudo-second-order adsorption (g mg^{-1} min^{-1}). Figure 6 showed pseudo-second-order kinetic model.

This article is an open access article distributed under the terms and conditions of the Creative Commons Attribution-NonCommercial 4.0 International (CC BY-NC 4.0 license) (http://creativecommons.org/licenses/by-nc/4.0/).

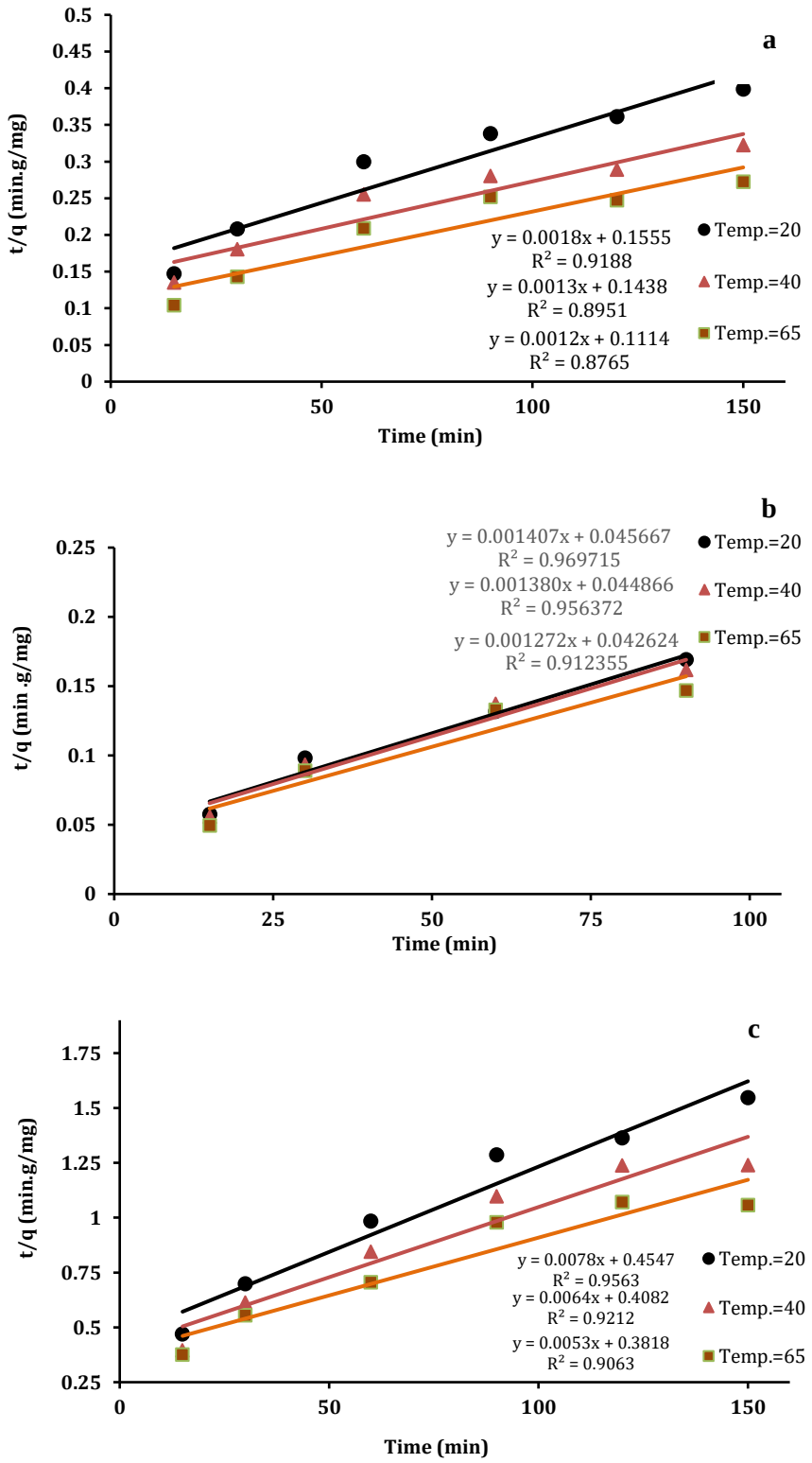

Figure 6: Pseudo-Second-Order kinetic plot for the adsorption of Pb(II) onto (a) I@Fe_3O_4 (b) II@Fe3O4 (c) III@Fe_3O_4 at different temp.

This article is an open access article distributed under the terms and conditions of the Creative Commons Attribution-NonCommercial 4.0 International (CC BY-NC 4.0 license) (http://creativecommons.org/licenses/by-nc/4.0/).

Table 8: Pseudo-Second-Order parameters for adsorption of Pb(II) onto prepared adsorbents at different temperature .

Absorbents	Temp. °C	Pb(II)		
		K_2	q_2	R_2^2
I@Fe_3O	20	2.083E-5	555.556	0.918
	40	1.175E-5	769.231	0.895
	65	1.292E-5	833.333	0.876
II@Fe_3O	20	3.791E-5	710.732	0.969
	40	4.244E-5	724.637	0.956
	65	3.795E-5	786.163	0.912
III@Fe_3O	20	1.338E-5	128.205	0.956
	40	1.035E-4	153.846	0.921
	65	7.357E-5	188.679	0.906

K_2 : (g mg^{-1} min^{-1}) , q : (mg / g) , Temperature : (°C)

The plots of linear form of the pseudo-first-order and pseudo-second-order for the adsorption of lead (II) ions onto adsorbents (I@Fe_3O_4 , II@Fe_3O_4 and III@Fe_3O_4) were obtained at the temperatures of 20°C, 40°C and 65°C respectively. The results of kinetic parameters were shown in Tables 7 and 8 above. The values of the correlation coefficients of the pseudo-first-order kinetic model (R_1^2) were higher than those of the (R_2^2) of the pseudo-second-order kinetic model . This indicates that the adsorption of lead (II) ions followed the pseudo-first-order kinetic with the correlation coefficients of higher than 0.99 for all tested temperatures.

3.7Adsorption Thermodynamics

Thermodynamic parameters consisting of Gibbs free energy change (ΔG°) , enthalpy change (ΔH°) and entropy change (ΔS°) were calculated from the following equation:

This article is an open access article distributed under the terms and conditions of the Creative Commons Attribution-NonCommercial 4.0 International (CC BY-NC 4.0 license) (http://creativecommons.org/licenses/by-nc/4.0/).

$$\Delta G^{\circ} = -RT \ln K_L \text{ .....(5)}$$

where R is the universal gas constant (8.314 $Jmol^{-1} K^{-1}$) , T is the temperature (K) , and K_L value was calculated using the following equation:

$$K_L = \frac{q_e}{C_e} \text{ ..... (6)}$$

where q_e and C_e are the equilibrium concentration of lead (II) ions onto the adsorbents (I@Fe_3O_4, II@Fe_3O_4 and III@Fe_3O_4) (mg g^{-1}) and in the solution (mg L^{-1}) , respectively. The enthalpy change (ΔH°) and entropy change (ΔS°) of the adsorption were estimated from the following equation:

$$\ln K_L = \frac{\Delta S^{\circ}}{R} - \frac{\Delta H^{\circ}}{RT} \text{ ..... (7)}$$

The enthalpy change (ΔH°) and entropy change (ΔS°) can be obtained from the slope and intercept of a Van't Hoff equation of (ΔG°) as follows :

$$\Delta G^{\circ} = \Delta H^{\circ} - T\,\Delta S^{\circ} \text{ ..... (8)}$$

where ΔG° is the Gibbs free energy change (KJ/mol) , thermodynamic parameters are listed in Table 9 . The Gibbs free energy change (ΔG°) is an indicator of the degree of the spontaneity in the adsorption process . In order to provide a better adsorption , it is necessary to have a negative value for the Gibbs free energy changes (ΔG°). The values of Gibbs free energy change (ΔG°) of lead (II) ions adsorption onto adsorbent I@Fe_3O_4 were determined as (- 1.233 , - 5.521and - 10.881) KJ mol^{-1} at the temperatures of 20°C , 40°C and 65°C respectively, The values of Gibbs free energy change (ΔG∘) of lead (II) ions adsorption onto adsorbent II@Fe_3O_4 were determined as (- 2.406 , - 4.665 and - 7.488) KJ mol^{-1} at the temperatures of 20°C, 40°C and 65°C respectively and the values of Gibbs free energy change (ΔG∘) of lead (II) ions adsorption onto adsorbent III@Fe_3O_4 were determined as (- 0.802 , - 3.459 and - 6.781) KJ mol^{-1} at the temperatures of 20°C, 40°C and 65°C respectively. These values indicate that the adsorption process is spontaneous and feasible under these conditions. The values of ΔG° at higher temperature are more negative than those of lower temperature . This means that high efficiency of adsorption takes place at high temperatures[11]. Plot of ln K_L versus 1/T for estimation of thermodynamic parameters for the adsorption of lead (II) ions onto adsorbents (I@Fe_3O_4 , II@Fe_3O_4 and

This article is an open access article distributed under the terms and conditions of the Creative Commons Attribution-NonCommercial 4.0 International (CC BY-NC 4.0 license) (http://creativecommons.org/licenses/by-nc/4.0/).

III@Fe_3O_4) is shown in Figure 7. The positive value of ΔS° reflects an increase in the degree of freedom of the adsorbent surface .

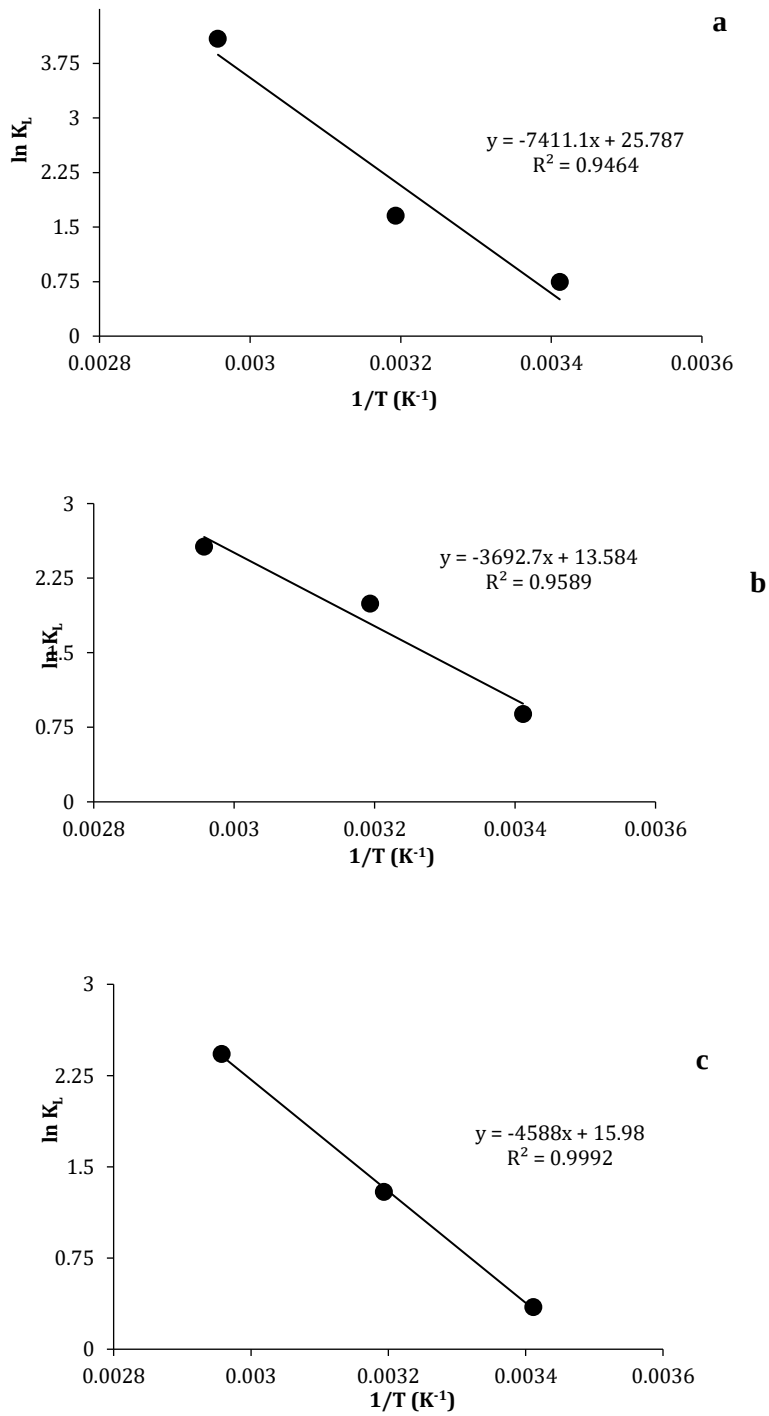

Figure 7: Plot of ln K_L versus 1 / T for estimation of thermodynamic parameters for the adsorption of Pb(II) onto (a) I@Fe_3O_4 (b) II@Fe_3O_4 (c) III@Fe_3O_4

This article is an open access article distributed under the terms and conditions of the Creative Commons Attribution-NonCommercial 4.0 International (CC BY-NC 4.0 license) (http://creativecommons.org/licenses/by-nc/4.0/).

Similar observation was reported in the literature[12] . The positive value of ΔH° for the adsorption of lead (II) onto adsorbents (I@Fe_3O_4 , II@Fe_3O_4 and III@Fe_3O_4) suggests an endothermic nature of process.

Table 9 : Thermodynamic parameters for adsorption of Pb(II) onto prepared adsorbents at different temperatures.

Adsorbant	Adsorbents	Temp. K	ΔH° *KJ/mole*	ΔS° *KJ/mole*	-ΔG° *KJ/mole*
Pb(II)	I@Fe_3O_4	293.15	61.615	0.214	1.233
		313.15			5.521
		338.15			10.881
	II@Fe_3O_4	293.15	30.701	0,112	2.406
		313.15			4.665
		338.15			7.488
	III@Fe_3O_4	293.15	38.144	0.132	0.802
		313.15			3.459
		338.15			6.781

3.8 Adsorption Isotherms

The adsorption data was analyzed with the use of Langmuir and Freundlich isotherms[13,14]. Langmuir isotherm :

$$\frac{C_e}{q_e} = \frac{1}{q_{max}K_L} + \frac{C_e}{q_{max}} \quad \text{..... (8)}$$

Where q_e is the equilibrium lead (II) ions concentration on the adsorbents (I@Fe_3O_4 , II@Fe_3O_4 and III@Fe_3O_4) (mg g^{-1}) respectively, C_e is the equilibrium lead (II) ions concentration in the solution (mg L^{-1}), q_{max} is the monolayer adsorption capacity of adsorbents (I@Fe_3O_4 , II@Fe_3O_4

This article is an open access article distributed under the terms and conditions of the Creative Commons Attribution-NonCommercial 4.0 International (CC BY-NC 4.0 license) (http://creativecommons.org/licenses/by-nc/4.0/).

and III@Fe_3O_4) (mg g^{-1}) respectively , and K_L is the Langmuir adsorption constant (L mg^{-1}) . The plots of C_e / q_e versus C_e for the adsorption of lead (II) ions onto the adsorbents (I@Fe_3O_4 , II@Fe_3O_4 and III@Fe_3O_4) are shown in Fig.8.

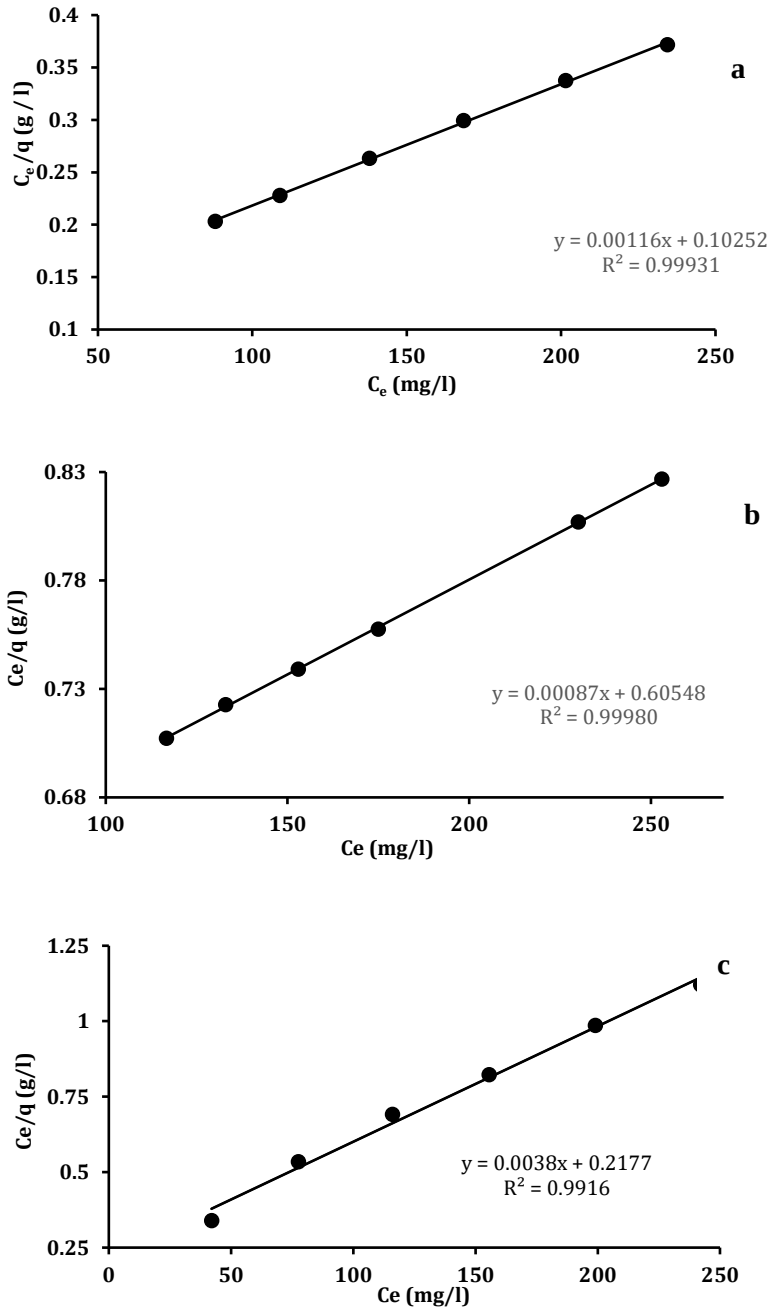

Figure 8: Langmuir adsorption isotherm of Pb(II) onto (a) I@Fe_3O_4 (b) II@Fe_3O_4 (c) III@Fe_3O_4 at 20°C .

This article is an open access article distributed under the terms and conditions of the Creative Commons Attribution-NonCommercial 4.0 International (CC BY-NC 4.0 license) (http://creativecommons.org/licenses/by-nc/4.0/).

Table 10: Langmuir isotherm parameters for adsorption of Pb(II) onto adsorbents at 20°C

Adsorbents	Adsorbant Pb(II)		
	q_{max}	K_L	R^2
I@Fe_3O_4	862.0689	0.01131	0.9993
II@Fe_3O_4	1149.425	0.00143	0.9998
III@Fe_3O_4	261.0966	0.01759	0.9880

K : (L / mg) , q_{max} : (mg / g)

Freundlich isotherm :

$$\log q_e = \log K_F + \frac{1}{n}\log C_e \quad \text{.....(10)}$$

where q_e is the equilibrium lead (II) ions concentration on the adsorbents (I@Fe_3O_4 , II@Fe_3O_4 and III@Fe_3O_4) (mg g^{-1}) respectively , C_e is the equilibrium lead (II) ions concentration in the solution (mg L^{-1}) and K_F (L g^{-1}) and n are the Freundlich adsorption isotherm constant. The plots of log q_e versus log C_e for the adsorption of lead (II) ions onto the adsorbents (I@Fe_3O_4 , II@Fe_3O_4 and III@Fe_3O_4) are shown in Figure 9. The Langmuir and Freundlich isotherm parameters are given in Tables 10 and 11 . The R^2 values of the Langmuir model is higher than that of the Freundlich model for I@Fe_3O_4 and II@Fe_3O_4 , but R^2 value of Freundlich model was more than Langmuir model for III@Fe_3O_4 . This lead to conclude that the adsorption of lead ions onto I@Fe_3O_4 and II@Fe_3O_4 were chemisorptions whereas the adsorption onto III@Fe_3O_4 was physiosorption. The Freundlich isotherm model suggests heterogeneous surface[15]. A comparison for lead (II) ion adsorption capacities of adsorbents (I@Fe_3O_4 , II@Fe_3O_4 and III@Fe_3O_4) produced from esters impregnated with iron oxide magnetic nanoparticales Fe_3O_4 is tabulated in Table 10. The maximum monolayer adsorption capacity of II@Fe_3O_4 from Langmuir isotherms for lead (II) ions is found to be the highest in comparison with the literature [16,17-23] .

This article is an open access article distributed under the terms and conditions of the Creative Commons Attribution-NonCommercial 4.0 International (CC BY-NC 4.0 license) (http://creativecommons.org/licenses/by-nc/4.0/).

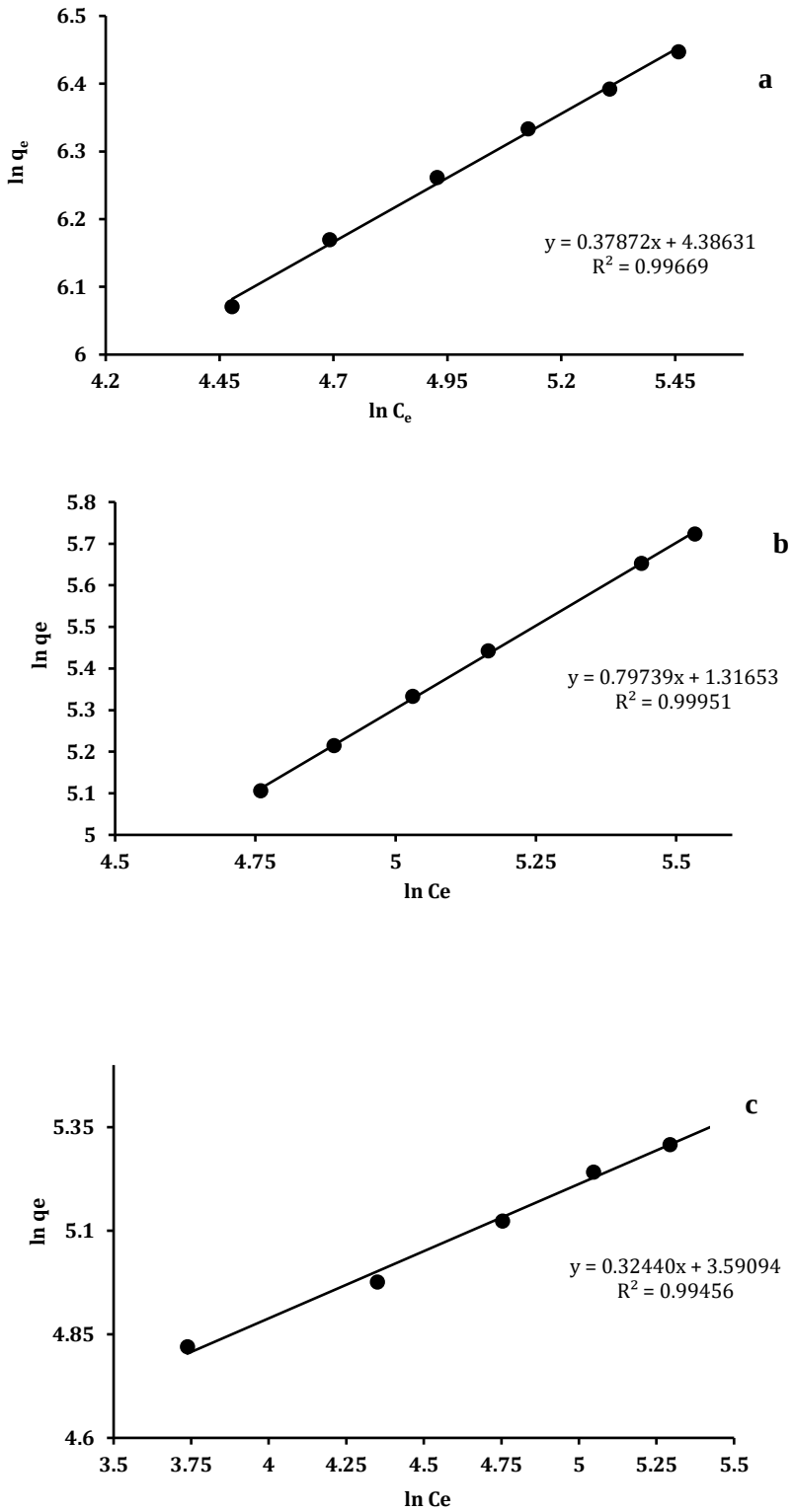

Figure 9: Freundlich adsorption isotherm of Pb(II) onto (a) I@Fe_3O_4 (b) II@Fe_3O_4 (c) III@Fe_3O_4 at 20° C .

This article is an open access article distributed under the terms and conditions of the Creative Commons Attribution-NonCommercial 4.0 International (CC BY-NC 4.0 license) (http://creativecommons.org/licenses/by-nc/4.0/).

Table 11: Freundlich isotherm parameters for adsorption of Pb(II) onto adsorbents at 20° C .

adsorbents	Adsorbant Pb(II)		
	K_F	1 / n	R^2
I@Fe_3O_4	80.342	0.378	0.996
II@Fe_3O_4	3.700	0.799	0.998
III@Fe_3O_4	39.409	0.307	0.9885

K : (L / mg)

4. Conclusions

Removal of lead ions from aqueous solution by the adsorbents (I@Fe_3O_4 , II@Fe_3O_4 and III@Fe_3O_4) produced from esters impregnated with iron oxide magnetic nanoparticales Fe_3O_4 has been carried out successfully. The main conclusions are as follows. The adsorption capacity for lead (II) ions was increased with an increase in the initial concentration of lead (II) ions. The kinetic modeling of the process followed the pseudo-first-order kinetic model at all tested temperatures . The R^2 values of the Langmuir model is higher than that of the Freundlich model for I@Fe_3O_4 and II@Fe_3O_4 , but R^2 value of Freundlich model was more than Langmuir model for III@Fe_3O_4 , and therefore this lead to conclude that the adsorption of lead ions onto I@Fe_3O_4 and II@Fe_3O_4 were chemisorptions whereas the adsorption onto III@Fe_3O_4 was physiosorption . The maximum monolayer adsorption capacity of the II@Fe_3O_4 was 1149.4252 mg g^{-1} which is quite high in comparison with the values in the literature.

This article is an open access article distributed under the terms and conditions of the Creative Commons Attribution-NonCommercial 4.0 International (CC BY-NC 4.0 license) (http://creativecommons.org/licenses/by-nc/4.0/).

References

[1] D. R. Baldwin , W. J. Marshall , Heavy metal poisoning and its laboratory investigation , Ann. Clin. Bio., 36 (1999) 267–300.

[2] F.U. Fenglian , Q. I. Wang, Removal of Heavy Metal Ions from Wastewater: A review , J. Envir. Manag. , 92 (2011) 407 – 418.

[3] Ph. Carson , C. Mumford , Hazardous Chemicals Handbook, Butterworth-Heinemann, 2nd edition, (2002).

[4] Lead poisoning and Health, World Health Organization (2021).

[5] D.A. Sahbas, A. Yakar, U. Gunduz, Magnetic Fe_3O_4 – chitosan micro – and nanoparticles for wastewater treatment, Partic. Sci. Tech. , 37 (2019) 732-74.

[6] H. Rashid, M.Adil Mansoor, B.Haider, R. Nasir, Sh.Bee Abd Hamid , A, Abdulrahman , Synthesis and characterization of magnetite nano particles with high selectivity using in-situ precipitation method, Sep. Sci. Techol., 55 (2020) 1207-1215.

[7] A.R. Sardarian , M. Zandi , S. Motevally , One – Pot Synthesis of Carboxlic Acid Ester in Neutral and Mild Condition by Triphenylphosphine Dihalide [ph_3PX_2 (X = Br , I)] , Acta. Chim. Slov., 56 (2009) 729 – 733 .

[8] M. Momcilovic , M. Purenovic , A. Bojic , A. Zarubica , M. Randelovid , Removal of lead(II) ions from aqueous solutions by adsorption onto pine cone activated carbon , Desalin. Water Treat., 276 (2011) 53–59 .

[9] A.A. Mizhir, A.A. Abdulwahid, H.S. Al-Lami, Adsorption of carcinogenic dye Congo red onto prepared graphene oxide-based composites, Desalin. Water Treat., 202 (2020) 381–395.

[10] A. A Abdulwahid, A.A. Alwattar, A. Haddad, M. Alshareef , J. Moore, S.G. Yeates , P. Quayle, An efficient reusable perylene hydrogel for removing some toxic dyes from contaminated water, Poly. Int., (2021) 1234-1245

[11] X.Y. Yu , T. Luo , Y.X. Zhang , Adsorption of lead(II) on O_2-plasma-oxidizedmultiwalled carbon nanotubes: thermodynamics, kinetics, and desorption , ACS Appl. Mat. Inter. , 3 (2011) 2585–2593.

[12] Z. Z. Chowdhury , S. M. Zain , R. A. Khan , R. F. Rafique , K. Khalid , Batch and fixed bed adsorption studies of lead (II) cations from aqueous solutions onto granular activated carbon derived from mangostana garcinia shell , Bioresour. , 7 (2012) 2895–2915.

This article is an open access article distributed under the terms and conditions of the Creative Commons Attribution-NonCommercial 4.0 International (CC BY-NC 4.0 license) (http://creativecommons.org/licenses/by-nc/4.0/).

[13] I. Langmuir , The adsorption of gases on plane surfaces of glass , mica and platinum , J. the Amer. Chem. Soc., 40 (1918) 1361–1403.

[14] H. M. F. Freundlich , Over the adsorption in solution , J. Phys. Chem., 57 (1906) 385-471.

[15] A. W. Adamson , Physical Chemistry of Surface , Inter science Publication , New York, NY, USA, 1960.

[16] M.M. Johns , W.E. Marshall , C. A. Toles , Agricultural byproducts as granular activated carbons for adsorbing dissolved metals and organics , J. Chem. Tech. Bio. , 71(1998) 131–140 .

[17] M. Kobya , E. Demirbas , E. Senturk , M. Ince , Adsorption of heavy metal ions from aqueous solutions by activated carbon prepared from apricot stone , Bioresour. Technol., 96 (2005) 1518–1521.

[18] R. R. Bansode , J. N. Losso , W. E. Marshall , R.M. Rao and R. J. Portier , Adsorption of metal ions by pecan shell-based granular activated carbons , Bioresour. Technol., 89 (2003) 115–119.

[19] Y. Kikuchi , Q. Qian , M. Machida and H. Tatsumoto , Effect of ZnO loading to activated carbon on Pb(II) adsorption from aqueous solution , Carbon , 44 (2006) 195–202 .

[20] G. Issabayeva , M. K. Aroua , N. M. N. Sulaiman , Removal of lead from aqueous solutions on palm shell activated carbon , Bioresour. Technol.,, 97, (2006) 2350–2355.

[21] R. Ayyappan , A. C. Sophia , K. Swaminathan , S. Sandhya , Removal of Pb(II) fromaqueous solution using carbon derived from agricultural wastes , Proc. Biochem., 40 (2005) 1293–1299 .

[22] V. Hoang, S. Nishihama, K. Yoshizuka, Selective adsorption of lead (II) from aqueous solution, Envron. Technol. , 17 (2020) 1-11.

[23] E. Koohzad, D. Jafari, H. Esmaeili, Adsorption of Lead and Arsenic Ions from Aqueous Solution by Activated Carbon Prepared from Tamarix Leaves, Chemist. Sel., 4 (2019) 12356-12367.

This article is an open access article distributed under the terms and conditions of the Creative Commons Attribution-NonCommercial 4.0 International (CC BY-NC 4.0 license) (http://creativecommons.org/licenses/by-nc/4.0/).

تحضير وتوصيف بعض الاسترات المشبعة بالجسيمات النانوية من اكسيد الحديد المغناطيسي Fe3O4 ودراسة كفاءتها في امتصاص ايونات الرصاص من محاليلها المائية

المستخلص

يعتبر عنصر الرصاص من العناصر السامة المتواجدة بشكل طبيعي على سطح الارض ، وقد أدى استخدامه على نطاق واسع إلى تلوث بيئي كبير حيث ان تعرض الانسان للرصاص يؤدي الى مشاكل كبيرة في الصحة العامة . في هذه الدراسة حضرت ثلاثة استرات مطعمة بدقائق اوكسيد الحيد النانوي المغناطيسي Fe_3O_4 . وهذه الاسترات حضرت من مفاعلة المركب الكحولي 2,2-bis(hydroxyl methyl)propane-1,3-diol مع الحوامض الكاربوكسيلية 4-hydroxy benzoic acid (I) و nicotinic acid (II) و stearic acid (III) ، ثم طعمت الاسترات الثلاثة المحضرة مع دقائق الحديد النانوية المغناطيسية Fe_3O_4 لتحضير ثلاث مواد مازة وهي I @ Fe_3O_4 و II @ Fe_3O_4 و III @ Fe_3O_4 ، ولقد اثبتت المواد المازة المحضرة أنها فعالة في إزالة أيونات الرصاص Pb(II) من المحاليل المائية عند دالة حامضية متعادلة تقريباً ، وكان سلوك الامتزاز مطابقًا لنموذج Langmuir لـ I @ Fe_3O_4 و II @ Fe_3O_4 (امتزازا كيمياوي) ومطابقاً مع نموذج Freundlich لـ III @ Fe_3O_4 (امتزاز فيزياوي) وبكفاءة امتزاز بلغت 862.068 mg / g و 1149.425 mg / g و 261.096 mg / g. للمواد المازة I @ Fe_3O_4 و II @ Fe_3O_4 و III @ Fe_3O_4 على التوالي . يتبع امتزاز Pb (II) حركية من الدرجة الاولى الزائفة لكافة انظمة الامتزاز لهذه الدراسة.

This article is an open access article distributed under the terms and conditions of the Creative Commons Attribution-NonCommercial 4.0 International (CC BY-NC 4.0 license) (http://creativecommons.org/licenses/by-nc/4.0/).